Frequency-Domain Characterization of Singular Spectrum Analysis Eigenvectors

Michel C. R. Leles*, Adriano S. V. Cardoso*, Mariana G. Moreira*, Homero N. Guimarães†,
Cristiano M. Silva*, Andreas Pitsillides§
*CELTA (Center for Studies in Electronics, Engineering and Automation), Universidade Federal de São João Del-rei
†Department of Electrical Engineering, Universidade Federal de Minas Gerais
‡Departmento de Tecnologia, Universidade Federal de São João Del-rei
§Department of Computer Science, University of Cyprus, Cyprus
Emails: {mleles,adrianosvc,marianageny}@ufsj.edu.br, hng@cpdee.ufmg.br
cristiano@ufsj.edu.br, andreas.pitsillides@ucy.ac.cy

***Abstract*—Singular Spectrum Analysis (SSA) is a nonparametric approach used to decompose a time series into meaningful components, related to trends, oscillations and noise. SSA can be seen as a spectral decomposition, where each term is related to an eigenvector derived from the trajectory matrix. In this context the eigenvectors can be viewed as *eigenfilters*. The frequency domain interpretation of SSA is a relatively recent subject. Although the analytic solution for the frequency-response of eigenfilters is already known, the periodogram is often applied for their frequency characterization. This paper presents a comparison of these methods, applied to eigenfilters' frequency characterization for time series components identification. To perform this evaluation, several tests were carried out, in both a synthetic and real data time series. In every situations the eigenfilters analytic frequency response method provided better results compared to the periodogram in terms of frequency estimates as well as their dispersion and sensitivity to variations in the SSA algorithm parameter.**

I. Introduction

Singular Spectrum Analysis (SSA) is a nonparametric approach firstly introduced by Broomhead & King [3]. It consists of a time series analysis technique able to be applied for distinct purposes in several knowledge fields [6].

Despite being a well-known and widely used tool, the frequency domain interpretation of the SSA is a relatively recent subject.

The periodogram is a Discrete Fourier Transform based spectral estimation method to frequency characterization of SSA eigenvectors in order to automatically select the cyclic components in the groping step. Using similar approach, Alexandrov [1] propose an algorithm to capture the trend components.

On the other hand, the relationship between SSA and filtering process has been addressed in some latter studies [6, 8, 2]. Harris & Yuan [8] showed that SSA methodology consists of a two-steps filtering process. The time series decomposition is achieved by the filtering with singular vectors obtained from the singular value decomposition of the trajectory matrix (eigenvectors). The eigenvectors consist of a set of eigenfilters. Complementarily, Kume [11] show that these eigenvectors compose a complete eigenfilters base, and SSA algorithm can be understood as a procedure of adjusting such eigenfilters in order to maximize the spectra of the filtered signals. Finally, Tome *et al.* [13] have provided an analytic solution for the frequency-response of SSA eigenvectors.

However, the periodogram is still applied to frequency characterization of the eigenfilters as can be seen in Ghanbarzadeh & Aminghafari [4], Mahdi *et al.* [12].

This paper provides a theoretical review of SSA method and frequency domain interpretation of eigenfilters. The analytic frequency-response and the periodogram of the eigenfilters obtained by SSA factorization are compared, in order to evaluate their performance for time series frequency components identification. To perform this assessment, several tests were carried out, in both synthetic and real data. In every situations the eigenfilters analytic frequency response method provided better results compared to the periodogram, in terms of frequency estimates as well as their dispersion and sensitivity to variations in the SSA algorithm parameter.

II. Methodology

The description presented in this section is based on Golyandina & Zhigljavsky [6]. The SSA method consists of two stages, concerning the decomposition and reconstruction of time series from the elementary matrices. The decomposition is accomplished by two sequential procedures: immersion and single value decomposition. The reconstruction process demands two more steps: grouping (selection of a subset of the elementary matrices) and diagonal averaging.

1) Immersion: Let $\mathbf{x} = (x_0, x_1, \cdots, x_n, \cdots, x_{N-1})^T$ represents the time series of length N of the signal under analysis. The time series may represent a continuous-time signal $x(t)$ sampled at rate $f_s = 1/T_s$ so that $x_n = x(nT_s) = x[n]$. The mapping of this signal into a matrix $\mathbf{A}$ of dimension $L \times K$, $L \leq K$, is called *immersion*, and it can be written as:

$$\mathbf{A} = \begin{bmatrix} x_0 & x_1 & \cdots & x_{K-1} \\ x_1 & x_2 & \cdots & x_K \\ \vdots & \vdots & & \vdots \\ x_{L-1} & x_L & \cdots & x_{N-1} \end{bmatrix}. \quad (1)$$

978-1-5090-5844-0/16/$31.00 ©2016 IEEE

L is the window length (embedding dimension), and $K = N - L + 1$. $\mathbf{A}$ is an *Hankel* matrix referred as the trajectory matrix [5].

2) Singular Value Decomposition: The factorization of the trajectory matrix $\mathbf{A}$ using Singular Value Decomposition (SVD) yields to:

$$\mathbf{A} = \mathbf{U}\mathbf{\Sigma}\mathbf{V}^T = \sum_{r=1}^{R} \sigma_r \mathbf{u}_r \mathbf{v}_r^T, \tag{2}$$

where $R = rank(\mathbf{A}) \leq L$. Matrix $\mathbf{U}$ is $L \times L$. Matrix $\mathbf{V}$ is $K \times K$. Both $\mathbf{U}$ and $\mathbf{V}$ are unitary rank matrices. $\mathbf{\Sigma}$, of dimension $L \times K$, is a diagonal matrix whose diagonal elements $\{\sigma_r\}$ are the singular values of $\mathbf{A}$. The eigenvalues of $\mathbf{A}\mathbf{A}^T$ are given by $\lambda_r = \sigma_r^2$. The columns of $\mathbf{U}$ and $\mathbf{V}$ form a set of orthonormal vectors. Columns of $\mathbf{U}$, or left singular vectors $\mathbf{u}_r$, are eigenvectors of $\mathbf{A}\mathbf{A}^T$, so that $\mathbf{A}\mathbf{A}^T\mathbf{u}_r = \lambda_r \mathbf{u}_r$ $(r = 1, \cdots, R)$. Columns of $\mathbf{V}$, or right singular vectors $\mathbf{v}_r$, are eigenvectors of $\mathbf{A}^T\mathbf{A}$, so that $\mathbf{A}^T\mathbf{A}\mathbf{v_r} = \lambda_r \mathbf{v}_r$ $(r = 1, \cdots, R)$. It can be shown that:

$$\mathbf{U}^T\mathbf{A} = \mathbf{U}^T\mathbf{U}\mathbf{\Sigma}\mathbf{V}^T = \mathbf{\Sigma}\mathbf{V}^T, \quad \text{and}$$
$$\mathbf{A}^T\mathbf{u}_r = \sigma_r \mathbf{v}_r. \tag{3}$$

The main components can be obtained by [15]:

$$\mathbf{w}_r = \sigma_r \mathbf{v}_r = \mathbf{A}^T\mathbf{u}_r, \tag{4}$$

where $\mathbf{w}_r$ is a $K \times 1$ vector. The $w_k^{(r)}$ elements of $\mathbf{w}_r$ are given by:

$$w_k^{(r)} = \sum_{l=0}^{L-1} u_l^{(r)}\, x_{l+k}, \quad k = 0, 1, \cdots, K-1, \tag{5}$$

where $u_l^{(r)}$ is $(l+1)$-th element of eigenvector $\mathbf{u}_r$ and $w_k^{(r)}$ is $(k+1)$-th element of the vector $\mathbf{w}_r$. The r-th elementary matrix, $\mathbf{A}_r$, an unitary rank $L \times K$ matrix, can be written as $\mathbf{A}_r = \sigma_r \mathbf{u}_r \mathbf{v}_r^T = \mathbf{u}_r \mathbf{w}_r^T$. It can be shown that $\|\mathbf{A}_r\|^2 = \sigma_r^2$ and

$$\|\mathbf{A}\|^2 = \sum_{r=1}^{R} \sigma_r^2, \tag{6}$$

where $\|.\|^2$ represents the Frobenius norm [5].

3) Grouping: Grouping is the procedure of arranging the r indices $\{1, 2, \cdots, R\}$ into M disjoint subsets I_m with $m = \{1, 2, \cdots, M\}$ and $I_m \subset \{1, 2, \cdots, R\}$. For the set of elementary matrices $\{\mathbf{A}_r \mid r \in I_m\}$, the resulting grouping matrix is:

$$\mathbf{A}_{I_m} = \sum_{r \in I_m} \mathbf{A}_r = \mathbf{A}_{\{.\}},$$

where $\{.\}$ designates the indices of I_m set.

The trajectory matrix can be rewritten as the sum of the M grouped matrices:

$$\mathbf{A} = \sum_{m=1}^{M} \mathbf{A}_{I_m}.$$

Each group is intended to represent an additive component of the time series (trend, oscillatory component, or noise) [9].

4) Diagonal Averaging: The purpose of this procedure is to recover the time series $\widetilde{\mathbf{x}}_r$ of length N from an elementary matrix $\mathbf{A}_r$ of dimension $L \times K$. One can calculate the diagonal averaging in N antidiagonals of $\mathbf{A}_r$ according to [15]:

$$\widetilde{\mathbf{x}}_n^{(r)} = \begin{cases} \frac{1}{n+1} \sum_{i=0}^{n} u_i^{(r)} w_{n-i}^{(r)} & \text{for } 0 \leq n < L-1, \\ \frac{1}{L} \sum_{i=0}^{L-1} u_i^{(r)} w_{n-i}^{(r)} & \text{for } L-1 \leq n < K, \\ \frac{1}{N-n} \sum_{i=n-K+1}^{N-K} u_i^{(r)} w_{n-i}^{(r)} & \text{for } K \leq n < N. \end{cases} \tag{7}$$

This procedure can be extended to any matrix resulting from the grouping process [5].

A. SSA Eigenvectors as Filters and their Frequency Responses

By analyzing Eqs. (4) and (5) one can notice that the vector $\mathbf{w}_r$ is the result of filtering the original time series $\mathbf{x}$ by a moving average filter (MA) whose coefficients are the elements of the eigenvector $\mathbf{u}_r$ in reverse order. Therefore, such eigenvector can be seen as an *eigenfilter* with transfer-function given by [7]:

$$F_r(z) = \sum_{l=0}^{L-1} u_{L-l}^{(r)} z^{-l} = \sum_{l=0}^{L-1} u_l^{(r)} z^{L-l}. \tag{8}$$

The procedure of diagonal averaging described by Eq. (7) for $L \leq n \leq K$ can be viewed as a second MA filter $G_r(z)$ whose coefficients are the elements of the eigenvector $\mathbf{u}_r$ in forward order. The transfer-function $G_r(z)$ is, thus, given by:

$$G_r(z) = \frac{1}{L} \sum_{l=0}^{L-1} u_l^{(r)} z^l. \tag{9}$$

The overall transfer-function of SSA technique is formed by the decomposition step described by filter $F_r(z)$ followed by the reconstruction step described by filter $G_r(z)$. Therefore, the SSA transfer function is the product of these two filters:

$$H_r(z) = F_r(z)\; G_r(z) = \frac{1}{L} \sum_{l=-(L-1)}^{L-1} \upsilon_l^{(r)} z^l. \tag{10}$$

As the coefficients of filters $F_r(z)$ and $G_r(z)$ are the same elements of $\mathbf{u}_r$ in forward and reverse order, the convolution sum is symmetric about the mean term [8]:

$$\upsilon_l^{(r)} = \upsilon_{-l}^{(r)},\; l = 1, 2, \cdots, L-1.$$

Actually, this symmetry results in a real-valued transfer-function with the associated frequency response [13]:

$$H_r(f) = \sum_{l=-(L-1)}^{L-1} \upsilon_l^{(r)} e^{j2\pi lf} = \upsilon_0^{(r)} + \sum_{l=1}^{L-1} 2\upsilon_l^{(r)} cos(2\pi lf). \tag{11}$$

Therefore, the two-step filtering of SSA decomposition and reconstruction produces a zero-phase response, which implies a zero delay between input and resulting signal [8]. The reconstruction of a series $\widetilde{\mathbf{x}}_r$ outside the $[L, K]$ interval, equation (7), can also be treated as the two-stage filtering with boundary effects [11].

Finally, Eq. (11) represents the analytic solution for the frequency response of SSA eigenfilters.

B. Periodogram

The periodogram $\mathcal{P}_x$ is an estimate of power spectral density from time series defined in [10] as:

$$\mathcal{P}_x\left(k/N\right) = \left|\sum_{n=0}^{N-1} x_n e^{-j2\pi kn/N}\right|^2 = \left|X_k\right|^2, \qquad (12)$$

where N is the length of the time series and X_k is the Discrete Fourier Transform (DFT) of the series $\mathbf{x}$:

$$X_k = \sum_{n=0}^{N-1} x_n e^{-j2\pi nk/N}, \quad 0 \leq k \leq N-1. \qquad (13)$$

An alternative definition for the periodogram is proposed by [1]:

$$\Pi_x(k/N) = \frac{1}{N}\begin{cases} 2\left|X_k\right|^2, & \text{for } 0 < k < N/2 \\ \left|X_k\right|^2, & \text{for } k = 0 \text{ or N is even and } k = N/2. \end{cases} \qquad (14)$$

This is done to ensure the following property:

$$\sum_{n=1}^{N} x_n^2 = \sum_{k=0}^{\lfloor N/2 \rfloor} \Pi_x(k/N), \qquad (15)$$

where $\lfloor . \rfloor$ represents the integer part of the division (floor).

C. Frequency Characteristics of SSA Eigenfilters

Eigenfilters frequency response can be estimated through the periodogram, a well-known Discrete Fourier Transform based method for spectral estimation. However, the periodogram frequency set is discrete and L-sized, where L is the length of time series and also the dimension of eigenfilter. It implies in a frequency resolution δ_f presented by [10]:

$$\delta_f = \frac{f_s}{L}\ . \qquad (16)$$

Small length eigenvectors frequency characterization can suffer with low spectral resolution, since very close frequency components cannot be discriminated, and their energy are spread between the closest frequencies belonging to the discrete set:

$$\{f_\Pi(k)\} = \left(0, \frac{1}{N}, \frac{2}{N}, \cdots, \frac{\lfloor N/2 \rfloor}{N}\right) f_s. \qquad (17)$$

On the other hand, the frequency response of a filter is completely determined by their coefficients. Therefore, Eq. (11) supplies an analytic way to determine eigenfilters frequency response in a continuous fashion.

D. Experimental Methods

In order to compare the frequency response of eigenvectors and the corresponding periodogram, a synthetic discrete-time series consisting of three frequency components with noise was generated, as described in Eq. (18):

$$\begin{aligned} y[n] =& A_1 \cos(2\pi(f_1+\gamma)nT_s) + A_2 \cos(2\pi(f_2+\gamma)nT_s) \\ &+ A_3 \cos(2\pi(f_3+\gamma)nT_s) + w[n], \end{aligned} \qquad (18)$$

where $w[n]$ denotes a zero-mean gaussian random-variable with variance calculated for a 10 dB signal-to-noise ratio. The γ factor was inserted to provide a controlled frequency deviation for a Monte Carlo experiment, later described in this section. In order to support the selection of the elementary matrices related to the harmonics series components, the eigenvalue spectra were computed.

The first experiment presents a graphic comparison of the selected eigenfilters frequency responses and their corresponding periodograms, for different embedding dimensions. In such case, the value of γ is zero. The eigenfilters' frequency responses were obtained through Eq. (11). The periodogram was computed through equation (14). The same analysis method were also applied to a time series of real data presented in section III-B.

A Monte Carlo simulation was conducted aiming the error estimation of both methods, in order to analyze their precision and accuracy. For these experiments, γ denotes a zero-mean, unitary-variance gaussian random variable. For each of the 500 iterations ran, a new value of γ is drawn; a new realization of the time series is generated; the frequency responses and periodograms of the selected eigenfilters are computed; the peak frequency is detected and registered, for both methods; and the resulting frequency deviation is calculated giving rise to Δ_F, for the frequency response method, and Δ_P, for the periodogram. These results are individually summarized in boxplots, for each frequency component, taking into account the embedding dimension adopted at the decomposition stage.

The boxplot representation was chosen due to their ability to display the dispersion in samples without making any assumptions of the underlying statistical distribution [14]. The median, first and third quartiles are shown in the box. The ends indicate minimum and maximum values, and outliers, when present, are depicted beyond these limits.

III. Results

As previously stated, we present assessments considering both synthetic and real data time series.

A. Synthetic Data

Fig. 1(a) shows an interval of the generated time series used in the following analysis. The chosen parameters in Eq. (18) were: $N = 2,000$ points; $T_s = 1$ ms; $A_1 = 2$; $A_2 = 1$; $A_3 = 1/2$; $f_1 = 11.5$ Hz; $f_2 = 30$ Hz and $f_3 = 36$ Hz.

Fig. 1(b) illustrates the eigenvalue spectra of σ_1 to σ_{10}. Three embedding dimensions were experimented: $L = 150$, $L = 180$ and $L = 1,000$.

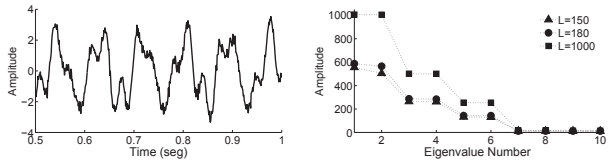

(a) Interval of time series $\mathbf{y}$. (b) Eigenvalues spectra

Fig. 1. (a) Synthetic time series generated by the addition of three sinusoidal components and white noise, for a 10 dB signal-to-noise ratio. (b) Eigenvalue spectra of σ_1 to σ_{10} for embedding dimensions $L = 150$, $L = 180$ and $L = 1,000$.

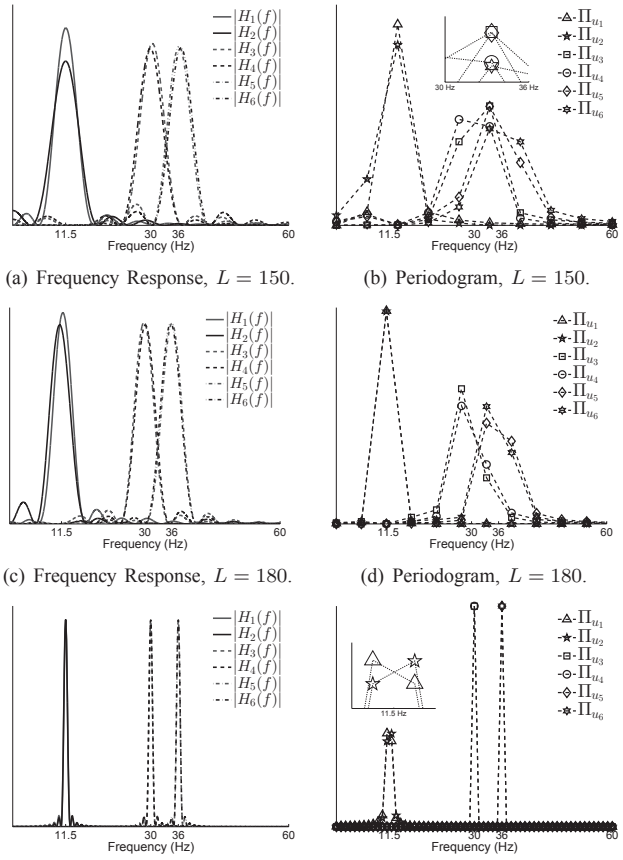

(a) Frequency Response, $L = 150$. (b) Periodogram, $L = 150$.

(c) Frequency Response, $L = 180$. (d) Periodogram, $L = 180$.

(e) Frequency Response, $L = 1000$. (f) Periodogram, $L = 1000$.

Fig. 2. Frequency characterization of the first six eigenvectors, obtained through frequency response and periodogram methods. The periodogram showed a poor frequency characterization for small window lengths due to the low spectral resolution.

Fig. 2 shows the comparison between the eigenvectors' frequency characterization through the frequency response method, (a), (c) and (e), and the periodogram, (b), (d) and (f). According to Eq. (16), the embedding dimensions L=150, L=180 and L=1,000 produce periodogram spectral resolutions of 6.67 Hz, 5.56 Hz, and 1 Hz, respectively. The frequency gap between the second and third harmonic time series components is 6 Hz.

Fig. 3 depicts the boxplots summarizing the comparison between frequency response and periodogram methods. 500 iterations of a random frequency deviation γ were ran. This procedure was repeated for the three adopted embedding dimensions. Figs. 3(a), 3(d) and 3(g) refer to the 11.5 Hz component; Figs. 3(b), 3(e) and 3(h) refer to the 30 Hz component; and Figs. 3(c), 3(f) and 3(i) to the 36 Hz.

B. Time Series of Real Data

The monthly Mediterranean Sea level is used as an example of a time series of real data. This non-stationary time series was analyzed by Mahdi *et al.* [12] using SSA, and is plotted in the Fig. 4, for Jan. 1993 to Oct. 2012.

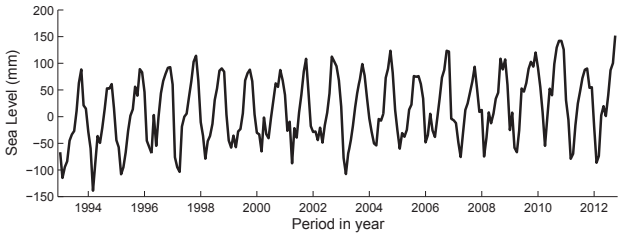

Fig. 4. Mediterranean Sea level fluctuation time series.

Mahdi *et al.* [12] employed an approach for automatic trend extraction and seasonal adjustment. They used the algorithm presented in Alexandrov [1] for trend detection, and the algorithm for performing automatic identification of harmonic components. The selected pairs of eigenvectors related to the harmonic components were: ($\mathbf{u}_1$, $\mathbf{u}_2$); ($\mathbf{u}_4$, $\mathbf{u}_5$); and ($\mathbf{u}_{32}$, $\mathbf{u}_{33}$), whose corresponding periods are 11.9725, 6.0035 and 2.2041 months, respectively. Authors employed the embedding dimension L=108.

In this work, two other values were adopted for comparison purposes ($L = 99$ and $L = 113$), in order to analyze the effects of this parameter on SSA eigenvector frequency characterization.

Fig. 5 depicts the SSA decomposition through eigenvectors frequency characterization for the sea level time series. Both eigenfilter frequency response and periodogram methods are shown for the selected L values.

IV. Discussion

The results obtained from both synthetic and real data time series showed that it is worth to apply the frequency response method for frequency characterization of SSA eigenfilters rather than periodogram.

The periodogram is a classic-and-well-known method for frequency-domain analysis, and so do their limitations. The spectral resolution depends upon the amount of data, and this is a drawback of such method. The maximum size for an eigenvector (L) is $N/2$ due to SSA decomposition constraints. Therefore, its spectral resolution is limited to $2f_s/N$ for the periodogram characterization.

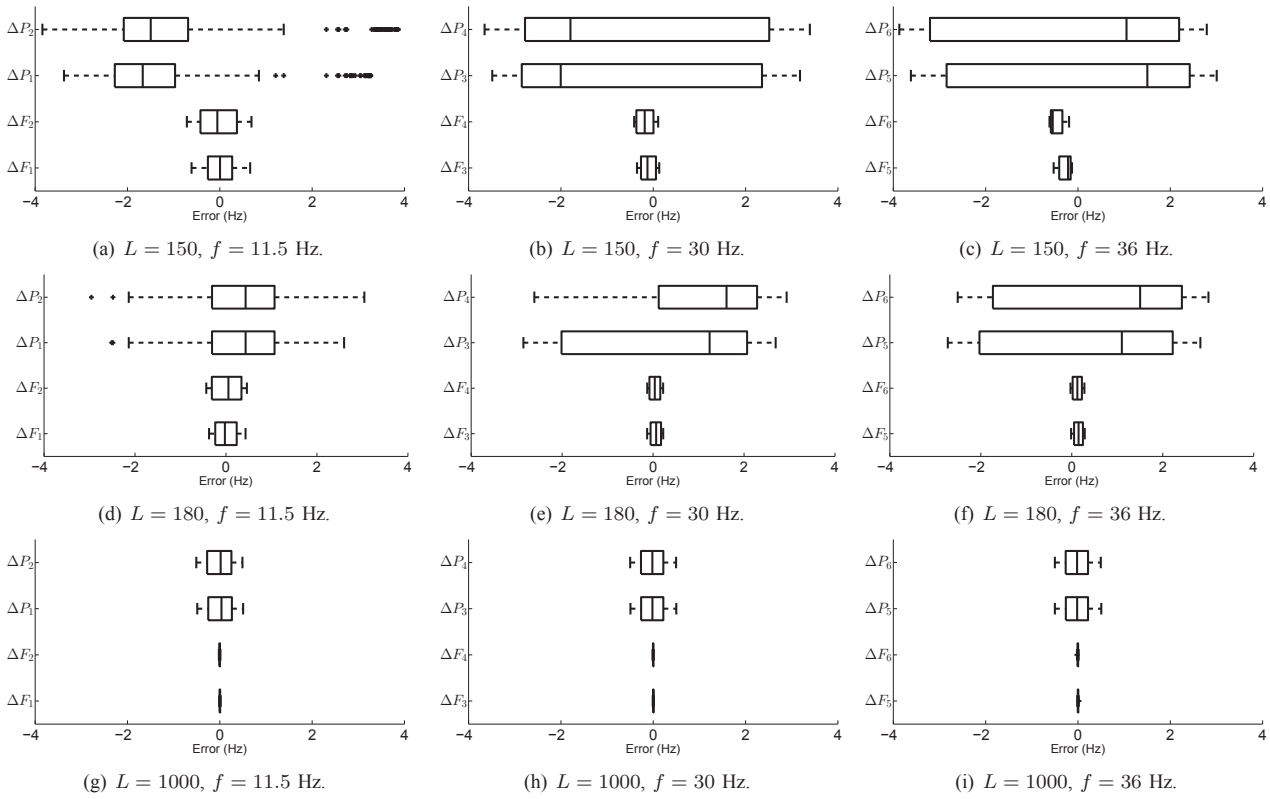

(a) $L = 150$, $f = 11.5$ Hz. (b) $L = 150$, $f = 30$ Hz. (c) $L = 150$, $f = 36$ Hz.

(d) $L = 180$, $f = 11.5$ Hz. (e) $L = 180$, $f = 30$ Hz. (f) $L = 180$, $f = 36$ Hz.

(g) $L = 1000$, $f = 11.5$ Hz. (h) $L = 1000$, $f = 30$ Hz. (i) $L = 1000$, $f = 36$ Hz.

Fig. 3. Boxplots showing the frequency error estimate dispersion for both periodogram and frequency response methods, for different window lengths. ΔP_k corresponds to the periodogram frequency error related to the $k-$th eigenfilter. ΔF_k corresponds to the frequency error related to the $k-$th eigenfilter obtained through the frequency response method. Data were produced by 500 iterations of a zero mean, unitary variance, normal distribution random frequency deviation γ. The absolute error is given by the difference between estimated and generated frequencies.

The frequency response approach for eigenfilters, conducts to an analytic solution for the frequency characterization. As a consequence, they do not suffer from spectral resolution problem. Fig. 2 exhibit this observation for the synthetic time series and Fig. 5 for the Mediterranean Sea level.

Actually, the eigenfilter frequency response becomes more precise as the embedding dimension increases, as can be noticed in both Figs. However, their peak value do not significantly departs from the frequency component it is attached to as the embedding dimension decreases.

In order to validate this observation, the frequency estimate error was analyzed using a Monte Carlo simulation and its result is summarized on Fig. 3. The boxplots reveal a important aspect of the proposed approach. In all situations, the frequency response method reached more accurate and also more precise results than the periodogram. Accuracy and precision of frequency estimates obtained from periodogram improve as the embedding dimensions increase. However, compared to the results achieved by the frequency response method, such improvement is subtle. Comparing the boxplots on Figs. 3(a) and 3(g); Figs. 3(b) and 3(h) and also in Figs. 3(c) and 3(i), it is easy to verify that the estimate frequency error performance achieved by the frequency response method, for $L = 150$, is close to that accomplished by the periodogram for $L = 1,000$.

Another important observation concerns the inherent discrete frequency of periodogram. Whenever a component frequency is not an integer multiple of the spectral resolution, a quantization error occurs. The worst case happens when its frequency is an odd integer multiple of half of the spectral resolution. Such case can be observed in Fig. 2 (f). The spectral resolution is 1 Hz, but the frequency component is an odd integer multiple of 0.5 Hz, 11.5 Hz. It can be noticed that both periodogram results, Π_{u1} and Π_{u2} were spread out over the interval between 11 Hz and 12 Hz.

A last observation regarding the sea level components characterization refers to the sensitiveness of the frequency characterization to the embedding dimension. Fig. 5 shows the frequency-domain characterization of eigenvectors $\mathbf{u}_1$, $\mathbf{u}_4$ and $\mathbf{u}_{32}$. As can be seen in Figs. 5(a)-5(c)-5(e), small variations of this parameter do not cause significant changes on the frequency distributions for the frequency response method.

On the other hand, such changes are much more noticeable in the periodogram (Figs. 5(b)-5(d)-5(f)). Similar results were found for eigenvectors $\mathbf{u}_2$, $\mathbf{u}_6$ and $\mathbf{u}_{33}$ (not presented here for the sake of brevity). The deviation of the frequency value relative to the peak caused by the variation of embedding dimension is visible for the periodogram method.

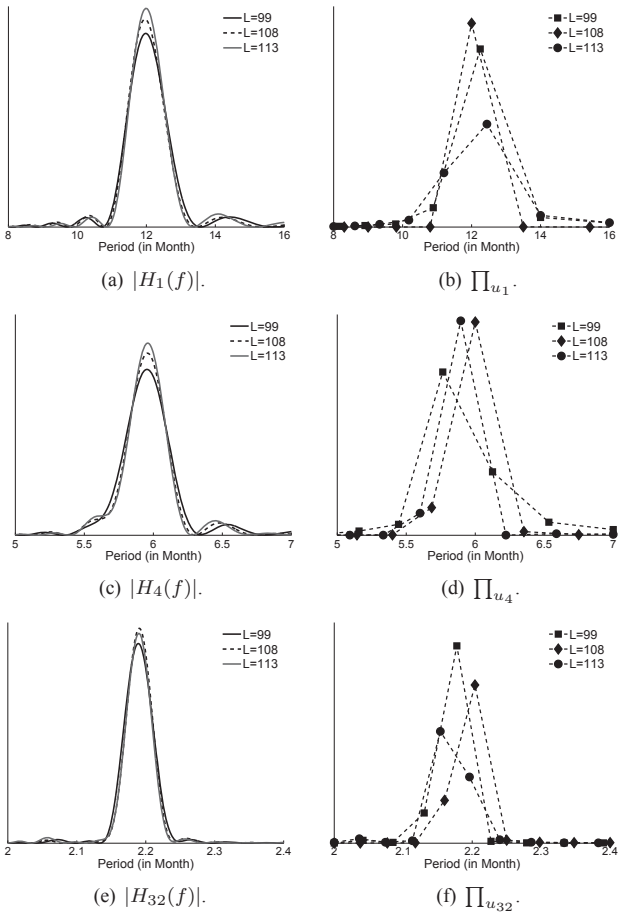

(a) $|H_1(f)|$. (b) $\prod_{u_1}$. (c) $|H_4(f)|$. (d) $\prod_{u_4}$. (e) $|H_{32}(f)|$. (f) $\prod_{u_{32}}$.

Fig. 5. Mediterranean Sea Level harmonic components detected by [12]: $\mathbf{u}_1$, 11.9725 months; $\mathbf{u}_4$, 6.0035 months; and $\mathbf{u}_{32}$, 2.2041 months. Periodogram vs. frequency response results for different embedding dimensions.

V. Final Remarks

Although an analytic solution for the frequency response characterization of SSA eingenfilters is known, Eq (11), the periodogram is still the standard frequency analysis tool currently applied for this purpose.

However, the theoretical analysis provided and the simulation results presented in this paper do not indicate the use of the periodogram in the frequency characterizations of SSA eigenfilters, since their analytic frequency response provide better results toward this end, in terms of frequency estimates as well as their dispersion and sensitivity to variations in the SSA embedding dimension parameter.

As future works, we are addressing a algorithm to use the analytic solution of eigenfilters frequency response, equation (11), rather than the periodogram to trend extraction and automatic detection of harmonic components.

Acknowledgments

This work was partially funded by FAPEMIG, CNPq, and CAPES.

References

[1] Alexandrov, T. (2009). A method of trend extraction using singular spectrum analysis. *REVSTAT - Statistical Journal* **7**(1), 1–22.

[2] Bozzo, E., Carniel, R. & Fasino, D. (2010). Relationship between Singular Spectrum Analysis and Fourier analysis: Theory and application to the monitoring of volcanic activity. *Computers and Mathematics with Applications* **60**, 812–820.

[3] Broomhead, D. S. & King, G. P. (1986). Extracting qualitative dynamics from experimental data. *Physica D* **20**(2-3), 217–236.

[4] Ghanbarzadeh, M. & Aminghafari, M. (2016). A new hybrid-multiscale ssa prediction of non-stationary time series. *Fluctuation and Noise Letters* **15**(1), 1650005.

[5] Golyandina, N., Nekrutkin, V. & Zhigljavsky, A. A. (2001). *Analysis of Time Series Structure: SSA and Related Techniques*. Chapman & Hall/CRC.

[6] Golyandina, N. & Zhigljavsky, A. A. (2013). *Singular Spectrum Analysis for Time Series*. Springer Briefs in Statistics.

[7] Hansen, P. C. & Jensen, S. H. (1998). FIR filter representations of reduced-rank noise reduction. *IEEE Transactions on Signal Processing* **46**(6), 1737–1741.

[8] Harris, T. & Yuan, H. (2010). Filtering and frequency interpretations of singular spectrum analysis. *Physica D* **239**, 1958–1967.

[9] Hassani, H. (2007). Singular spectrum analysis: Methodology and comparison. *Journal of Data Science* **5**(2), 259–267.

[10] Kay, S. & Marple, J., S.L. (1981). Spectrum analysis - a modern perspective. *Proceedings of the IEEE* **69**(11), 1380–1419.

[11] Kume, K. (2012). Interpretation of Singular Spectrum Analysis as complete eigenfilter decomposition. *Advances in Adaptive Data Analysis* **04**(04), 1250023.

[12] Mahdi, H., Hassani, H. & Taibi, H. (2013). Sea level in the Mediterranean Sea: seasonal adjustment and trend extraction within the framework of SSA. *Earth Science Informatics* **06**(02), 99–111.

[13] Tome, A. M., Teixeira, A. R., Figueiredo, N., Santos, I. M., Georgieva, P. & Lang, E. (2010). SSA of biomedical signals: A linear invariant systems approach. *Statistics and Its Interface* **3**, 345–355.

[14] Tukey, J. W. (1977). *Exploratory Data Analysis*. Addison Wesley.

[15] Vautard, R., Yiou, P. & Ghil, M. (1992). Singular-Spectrum Analysis: A toolkit for short, noisy chaotic signals. *Physica D* **58**, 95–126.